SI-2022PMTGE:

Evaluation of heavy roller compaction on large thickness layer of subgrade with full-scale field experiments

Shu-jian WANG[1,3], Hong-guang JIANG[1], Zong-bao WANG[2], Yu-jie WANG[1], Yi-xin LI[1,4], Xue-yu GENG[4], Xin-yu WANG[1], Kai WANG[5], Yi-yi LIU[1], Yan-kun GONG[1]

[1]*School of Qilu Transportation, Shandong University, Jinan 250002, China*

[2]*Shandong Hi-Speed Engineering Test Co., Ltd., Jinan 250002, China*

[3]*Shandong High-Speed Jiqing Middle Line Highway Co., Ltd., Gaomi 261599, China*

[4]*School of Engineering, University of Warwick, Coventry CV48UW, UK*

[5]*Shandong Hi-speed Group Co., Ltd, Jinan 250002, China*

Abstract: Subgrade construction is frequently interrupted due to the precipitation, soil shortage and environmental protection. Therefore, increasing the thickness layer is necessitated to reduce construction costs and allow highways to be placed into service earlier, thus reducing the required operating time and fuel consumption, which implies lower costs and environmental impact. This paper presented a series of full-scale field experiments to evaluate the compaction quality of gravel subgrade with large thickness layers of 65 cm and 80 cm via heavy vibratory rollers. Improved sand cone method was first proposed and calibrated to investigate the distributions of soil compaction degree along the full subgrade depth. Dynamic soil stresses, accumulative settlement, indicators of subgrade bearing capacity were measured with the roller passes, and their correlations with compaction degree were then analyzed to provide criterions to evaluate the compaction quality. Results showed that dynamic soil stresses caused by the heavy vibratory rollers were 2.4~5.9 times larger than those of traditional rollers, especially at deeper depths, which were large enough to densify the soils in the full depth. A unified empirical formula was proposed to determine the vertical distribution of dynamic soil stresses caused by roller excitation. It was demonstrated that soils were effectively compacted in a uniform fashion with respect to the full depth to 96%~97.2% and 94.1%~95.4% for the large thickness layers of 65 cm and 80 cm within limited 6~7 passes. Moreover, heavy roller compacted subgrade with large thickness layers had equivalent even better bearing capacity than that of conventional compaction thickness. Empirically linear formulae were finally established between soil compaction degree and subgrade reaction modulus, dynamic modulus of deformation, dynamic deflection and relative difference of settlement to conveniently evaluate the compaction qualities. Therefore, increasing thickness layer via heavy rollers could significantly reduce the cost and time burdens involved in construction while ensuring overall subgrade quality.

Key words: Highway subgrade; Heavy vibratory roller; Thickness layer; Dynamic soil stress; Compaction degree; Compaction quality control

1 Introduction

Subgrade should have sufficient compaction degree and bearing capacity to support the upper structures and vehicles. However, the subgrade construction is frequently interrupted due to the precipitation, soil shortage and environmental protection in China. Consequently, the remaining time is quite limited for the subgrade engineering which is commonly compacted in layers with 30 cm thick or less. Therefore, it is imperative to accelerate the construction schedule of subgrade engineering. Although rollers of more than 30 tons have gradually been utilized in the field work, making it possible to compact soil layers thicker than 30 cm, efficient technologies and credible detection methods are still ambiguous to guarantee the soil compaction quality of the full depth of subgrade.

To increase the thickness layer of subgrade compaction, construction machineries with large excitation force were first manufactured. Kim et al. (2016) inferred that the impact rollers seemed to have more potential for use in final compaction of thicker layers. Through rapid impact construction (RIC), Mohammed et al. (2013) found that the compaction degree of silt sand was improved from 45% to 70% with the maximum thickness of 5.0 m. Ghanbari et al. (2014) showed that RIC strongly improved the soil up to 2 m in depth and commonly influenced the soil up to depths of 4 m. However, RIC method generates discrete tamping points, which is difficult to ensure the uniformity of subgrade compaction. Xu et al. (2013) validated the performance of the IR technology, in order to compact subgrade continuously, impact roller compaction (IRC) was successfully applied to subgrade compaction due to the larger impact force. Although the IRC method is capable to compact deeper soils, the compaction degree of soils within the upper 0.5 m is always non-uniform. Chen et. al. (2021) validated the developed numerical scale model against a field study using the full-size Rolling dynamic compaction (RDC) module. Nowadays, heavy-weight (more than 26 tons) vibratory roller compaction (VRC) has been widely used in subgrade construction. With larger eccentric force and deeper reinforcement depth, it is possible to compact subgrade with greater thickness layer. Mooney et. al. (2007) pointed out that the influencing depth of VRC was affected by soil stiffness and the coupled dynamic effect of roller and soil. Moreover, Wersaell et al. (2013) conducted 85 small-scale tests and found that there was a distinct frequency dependence, implying a significantly improved compaction effect close to the compactor–soil resonant frequency. Wersaell et al. (2017) conducted a full-scale test and found that lower compaction frequency significantly reduced the required engine power and thus fuel consumption and environmental impact, while increasing the lifespan of the roller. Wersaell et al. (2018) confirmed that the lower frequency was more efficient for compaction and that utilizing resonance in the roller-soil system could reduce the number of passes. Moreover, Wersaell et al. (2020) proposed that crushed gravel of 100 cm thick could be dramatically better compacted by vibratory roller under the resonant frequency of the coupled compactor-soil system, while the efficiency increased by about 20%. Chen et al. (2019) studied the construction technology of rock materials using a roller of 32 tons and pointed out that it was effectively compacted within the depth of 90 cm. Furthermore, the automatic frequency conversion compaction technology was successfully applied on the construction site, and a vibratory roller of 20.9 tons could effectively reinforce crushed rock of 1 m.

Since the maximum detection thickness of compaction degree is less than 400 mm as stipulated in the Chinese specification (JTG 3450- 2019), it is necessary to propose a reliable testing method to suit the large thickness layer. Cui (2010) found that the pore pressure and soil stress were stabilized with the number of compactions, and correlated well with the compaction state. Xu (2021) combined the geological radar with sand filling method, and detected the compaction state along the depth. Based on the analysis of dynamic impact and vibration waves, Zhang et al. (2021) proposed that the layered interface settlement (LIS) of subgrade changed significantly at the bounded depth of 0.9m. Li at al. (2020) proposed that the resistivity method could be used for moisture detection, while the polarizability method was suitable for compaction measurement. Yuan et al. (2020) conducted the electrical measuring in laboratory and found the exponential/logarithmic relationship among the water content, compaction degree or the polarizability. Generally, falling weight deflectometer (FWD) system could reflect the compaction state of soil by measuring its impact load and the deflection of the plate. Sulewska (2012) pointed out that the compaction degree of non-cohesive soil could be well detected by the light falling weight deflectometer (LFWD) method. Furthermore, Vennapusa et al. (2009) provided a review of basic principles, different manufacturer LWD equipment. Fujyu et al. (2004) introduced the techniques used in the load and the deflection measurements in the FWD-light system. Vennapusa et al. (2012) proposed that the influence depth of Falling Weight Deflectometer (FWD) and Light Weight Deflectometer (LWD) were 60 cm and 30 cm, respectively.

Current researches were mainly focused on the construction technology of VRC and the measurement of modulus or deflection at subgrade surface. Although the VRC method could increase the subgrade thickness layer, the uniformity of the compaction degree along subgrade depth was rarely evaluated as well as its relationships with other indices. In this paper, a series of full-scale field experiments were carried out on the thickness layers of 65 cm and 80 cm with heavy roller compaction, in comparison to the traditional thickness layer of 30 cm. The sand cone method was improved to determine the soil compaction degree for the full subgrade depth. Soil pressure sensors were embedded at different depths to record the dynamic soil stresses caused by moving rollers. An empirical formula was proposed to determine the distribution of dynamic soil stresses along soil depths. In order to assess the compaction quality, the subgrade settlement (S), subgrade reaction modulus (K_{30}), dynamic modulus of deformation (E_{vd}) and dynamic deflection (L) were also measured after each roller pass. Relationships between these indices were further analyzed to reliably evaluate the effects of heavy roller compaction on large thickness layer of subgrade.

2 Full-scale field experiment

2.1 Materials

To evaluate the influence of thickness layer on the compaction effect of the subgrade soil, a full-scale field experimental program was designed and tested in the Weifang-Qingdao Expressway in Shandong Province, China. Sieve tests were carried out to determine the particle distribution characteristics of the subgrade filling material as shown in Fig. 1. The filling material was poor-graded gravel (GP) with coefficient of uniformity C_u=107.7 and coefficient of curvature C_c=0.15.

Due to the dimension limitation of the testing tube relative to the maximum particle size of the filling material, the maximum dry density (bulk density) was determined by the similar gradation method with four different particle-size ratios of 2, 3, 6 and 12 as specified in the Chinese Standard of Test Methods of Soils for Highway Engineering (JTG 3430-2020). Each group of the dry filling material was prepared by the vibration compaction method to reach its maximum dry density as shown in Fig. 2(a) according to the Standard. Then a logarithmic formula could be fitted based on the experimental values of the maximum dry density with four different particle-size ratios. Based on this empirical formula as shown in Fig. 2(b), the maximum dry density of the field filling material was determined to be 2.216 g/cm^3 as the particle-size ratio equal to 1.0.

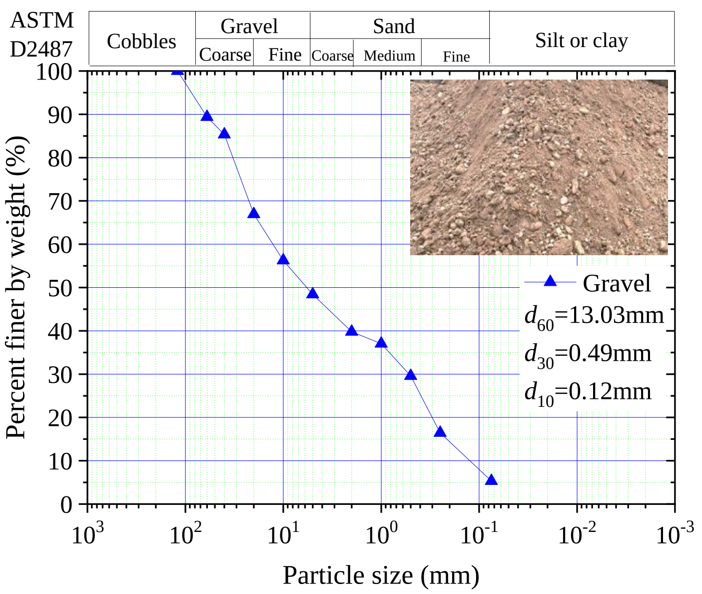

Fig. 1 Particle distribution characteristics of the subgrade filling

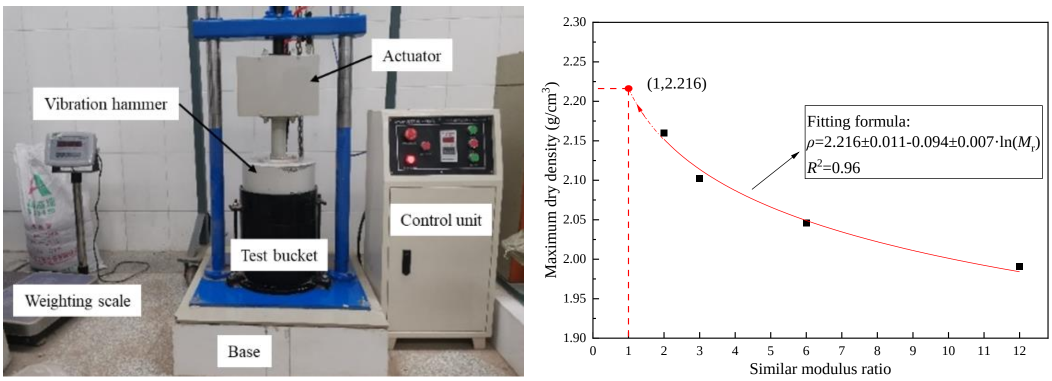

(a) Surface vibration compaction instrument **(b) Similar gradation method**

Fig. 2 Maximum dry density test of the subgrade filling

2.2 Program of full-scale field experiment

The full-scale field experiment was carried out in three test sections with different thickness layers. Two large thickness layers of 65 cm (TS-65) and 80 cm (TS-80) were selected to evaluate the subgrade compaction quality, and the conventional thickness layer of 30 cm (TS-30) was used as the control group. Each test section was 200 m long and 50 m wide, which was compacted with the same subgrade filling material (GP). Two types of smooth-drum vibration rollers (XuGong XS263J and ZhongDa YZ362) were adopted to optimize the compaction technology combination. The main roller technical parameters are shown in Table 1. The total weight of the XuGong XS263J roller is 26 t with a drum width of 3.28 m, which can provide vibration frequencies of 27 Hz and 32 Hz, corresponding to the exciting forces of 290 kN and 405 kN. The roller of ZhongDa YZ362 has a large-tonnage weight of 36 t with a drum width of 3.4 m. Since this roller is equipped with the stepless frequency modulation hydraulic system, it can provide vibration frequencies from 0 to 28 Hz. During the field compaction, two commonly used frequencies of 21 Hz and 24 Hz were selected to output 500 kN and 700 kN excitation force, respectively.

Table 1 Main roller technical parameters

Parameter	Value	
	XuGong XS263J	ZhongDa YZ362
Total operation mass (kg)	26000	36000
Static load (N/cm)	582	1040
Excitation frequency (Hz)	27/32	0~28
Excitation amplitude (mm)	1.9/0.95	2.0
Eccentric force (kN)	405/290	360~800
Drum width (mm)	3280	3400

In order to satisfy the required thickness layer of each compaction layer, the volume of subgrade filling material was first estimated per unit grid of 1 m×1 m. Therefore, the test section was gridded and filled with the required volume of subgrade filling material. Steel bars were embedded around the boundaries of the subgrade as a reference to the target thickness, which was implemented by the grader machine. The rolling process was then carried out to compact the subgrade filling material with certain excitation forces and rolling passes. Table 2 lists detailed compaction parameters of the three test sections. For the cases of TS-65 and TS-80, the soil layer was first pre-compacted by a XS263J Roller to provide a relatively firm working surface, otherwise the roller with higher excitation force was likely to be trapped in the thick uncompacted soil layer. Then the soil layer was compacted by two passes of YZ362 Roller of 700 kN, followed by two passes and three passes of 500 kN excitation forces for the TS-65 and TS-80 at the speed of 1.0 m/s, respectively. For comparison, the soil layer of TS-30 was first compacted by two passes of YZ362 Roller of 500 kN, followed by three passes of XS263J Roller of 290 kN. Finally, the rolling surface was flattened by the grader machine and complementally compacted by XS263J Roller without vibration.

Table 2 Compaction process of each test section

Test Section	Thickness layer	1^{st} Pass	2^{nd} Pass	3^{rd} Pass	4^{th} Pass	5^{th} Pass	6^{th} Pass	7^{th} Pass

TS-65	65 cm	XS263J Roller 0 Hz/ 260 kN	YZ362 Roller 700 kN/ 24 Hz	YZ362 Roller 700 kN/ 24 Hz	YZ362 Roller 500 kN/ 21 Hz	YZ362 Roller 500 kN/ 21Hz	XS263J Roller 0 Hz/ 260 kN	-
TS-80	80 cm	XS263J Roller 0 Hz/ 260 kN	YZ362 Roller 700 kN/ 24 Hz	YZ362 Roller 700 kN/ 24 Hz	YZ362 Roller 500 kN/ 21 Hz	YZ362 Roller 500 kN/ 21 Hz	YZ362 Roller 500 kN/ 21 Hz	XS263J Roller 0 Hz/ 260 kN
TS-30	30 cm	YZ362 Roller 500 kN/ 21 Hz	YZ362 Roller 500 kN/ 21 Hz	XS263J Roller 405 kN/ 27 Hz	XS263J Roller 405 kN/ 27 Hz	XS263J Roller 405 kN/ 27 Hz	XS263J Roller 0 Hz/ 260 kN	-

Soil pressure caused by rollers is considered as a direct parameter to reflect the compaction influencing depth. During rolling compaction, dynamic soil stresses along the layer depth were measured by soil pressure transducers, which were calibrated in laboratory before installation in the full-scale field experiment. Fig. 3 illustrates the configurations of the embedded soil pressure transducers at different depths with a spacing of 0.5 m in the longitudinal direction. As shown in Fig. 4, the periphery of soil pressure transducers was filled with compacted standard sand to uniformly transmit the roller induced dynamic soil stresses. A data acquisition instrument was adopted to record the time-history information of dynamic soil stresses with the sampling frequency of 1000 Hz.

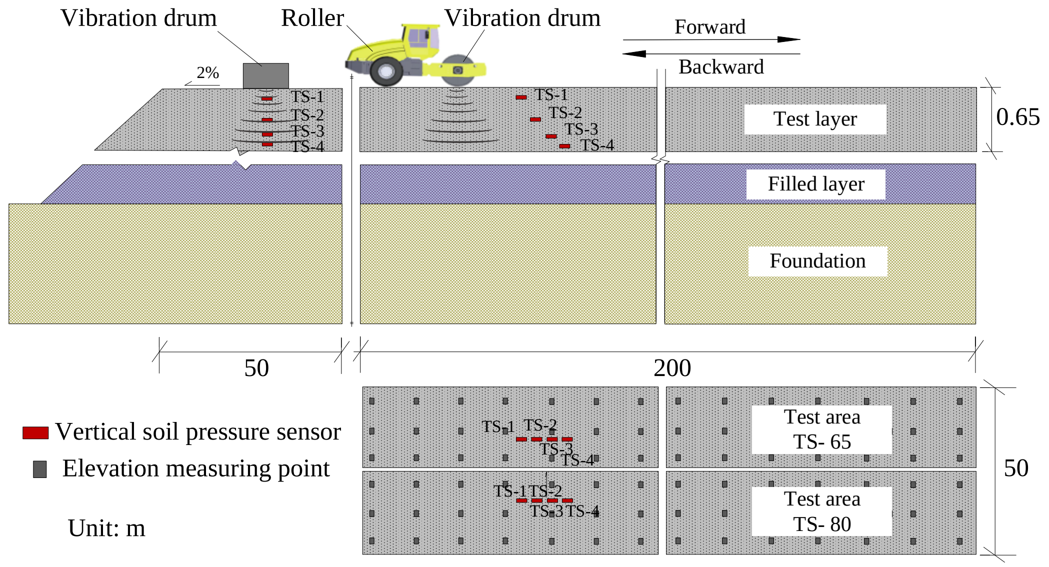

Fig. 3 General view of test sections: cross section and longitudinal section

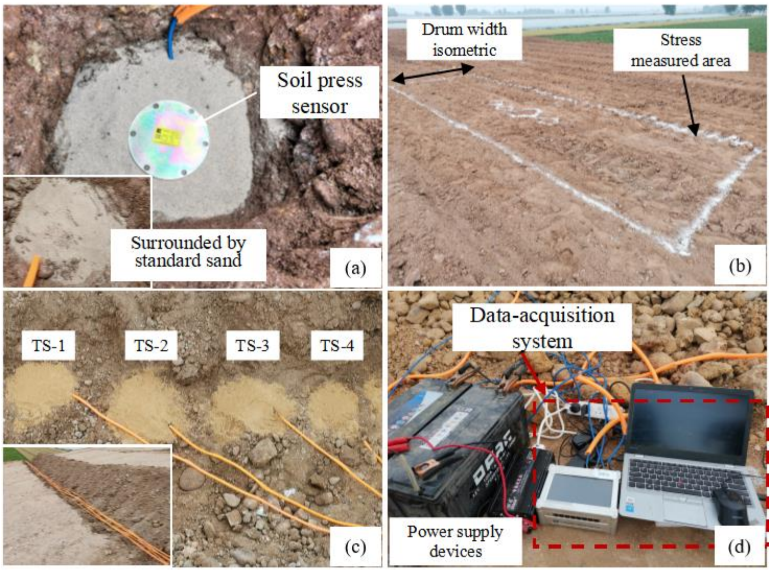

Fig. 4 Installation of soil pressure transducers

In order to assess the compaction quality, the subgrade settlement (S), compaction degree (K), subgrade reaction modulus (K_{30}), dynamic modulus of deformation (E_{vd}), and dynamic deflection (L) of each compacted layer were measured after each roller pass, respectively. The test methods, formulae, type of instrument and boundary requirements of S, K and L refer to the Chinese specification (JTG 3450- 2019), while those of K_{30} and E_{vd} refer to the Chinese specification (TB 10751 - 2018). The compactness tests for each compacted layer were conducted with an improved sand cone method. Details about the improved sand cone method are described in the attachment.

In order to investigate the distribution of soil compactness along the compacted layer for the thickness layers of 65 cm and 80 cm in the field experiments, the sand cone tests were conducted at three different depths of the compacted layer for each roller pass, i.e., the upper layer (0~1/3 depth from the compacted layer surface), middle layer (1/3~2/3 depth) and bottom layer (the remaining 1/3 depth from the compacted layer bottom). Fig. 5 illustrates the test procedures of the sand cone method. To facilitate the field measurement, the soil compactness at three different depths was implemented within the same testing pit. And the soil compactness can be calculated by the following formulae:

$$K_{\mathrm{i}} = \frac{m_{\mathrm{fd,i}}}{\frac{m_{\mathrm{s,i}}}{\rho_{\mathrm{s,i}}} - \frac{m_{\mathrm{s,i-1}}}{\rho_{\mathrm{s,i-1}}}} \cdot \frac{1}{\rho_{\mathrm{d,max}}} \times 100\% \quad (1)$$

$$m_{\mathrm{s,0}} = 0 \quad (2)$$

where i = 1, 2 and 3, represents the upper, middle and bottom layer, respectively; $\boldsymbol{m}_{\mathbf{fd,i}}$ is the dry mass of the subgrade filling at i^{th} layer; $\boldsymbol{\rho}_{\mathbf{d,max}}$ is the maximum dry density of the subgrade filling; $\boldsymbol{m}_{\mathbf{s,i}}$ is the mass of falling sand at i^{th} layer; $\boldsymbol{\rho}_{\mathbf{s,i}}$ is the density of falling sand at i^{th} layer, which is detailed in the attachment.

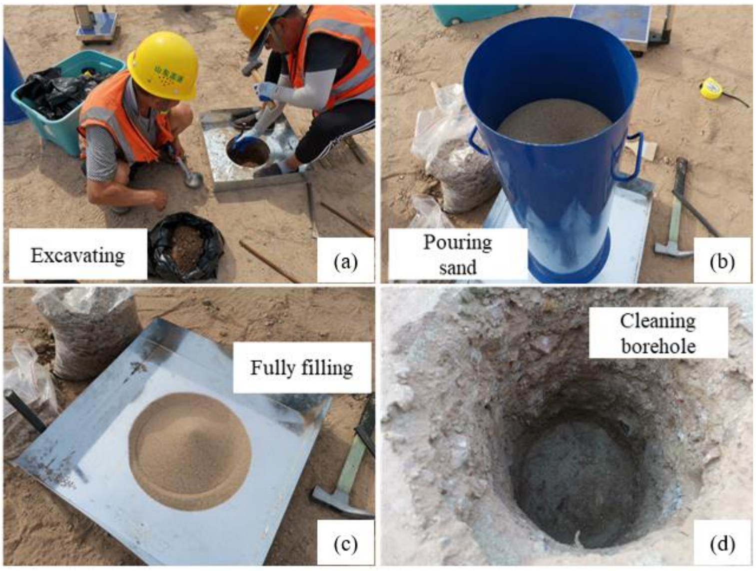

Fig. 5 Test procedures of the sand cone method in the field experiment

The static rigidity of the compacted subgrade was evaluated by the subgrade reaction modulus K_{30} via a rigid plate of 30 cm in diameter as shown in Fig. 6(a). The applied stress and induced displacement were recorded during the staged loading. And the K_{30} value was determined by the applied stress by the following formula:

$$K_{30} = \frac{\sigma_s}{\Delta l} \tag{3}$$

where σ_s is the applied stress on the rigid plate corresponding to the displacement of 1.25 mm, MPa; Δl is the displacement valued 1.25 mm here. Besides, the dynamic rigidity of the compacted subgrade was further evaluated by the dynamic deflection L using the Falling Weight Deflectometer (FWD, see Fig. 6(b)) and the dynamic modulus of deformation using the Portable Falling Weight Deflectometer (PFWD, see Fig. 6(c)).

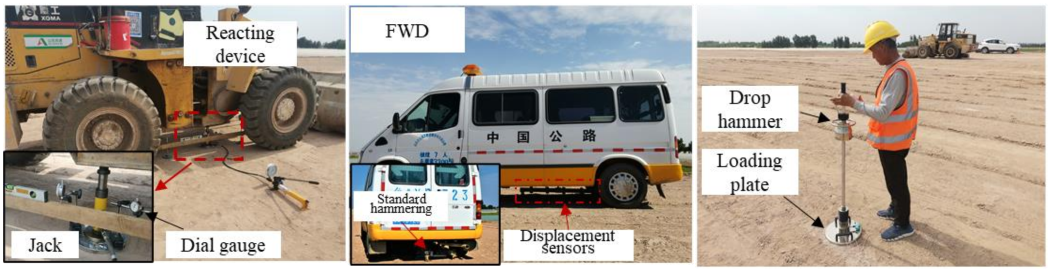

(a) K_{30} test **(b) FWD test** **(c) PFWD test**

Fig. 6 In situ measurement

3 Test Results and Analysis

3.1 Dynamic soil stress

Typical time history and frequency spectrum curves of measured dynamic soil stresses caused by the moving roller are illustrated in Fig. 10, taking the YZ362 Roller vibrating at 24 Hz at the depth of 37 cm as an example. Two main peaks in Fig. 7(a) correspond to the vibratory drum and the followed non-vibratory wheel, with the maximum values of 0.46 MPa and 0.07 MPa, respectively. Considering the peak value of 24 Hz from the frequency spectrum analysis in Fig. 7(b), it can be found that the compaction energy is mainly contributed from the drum vibration rather than its static weight.

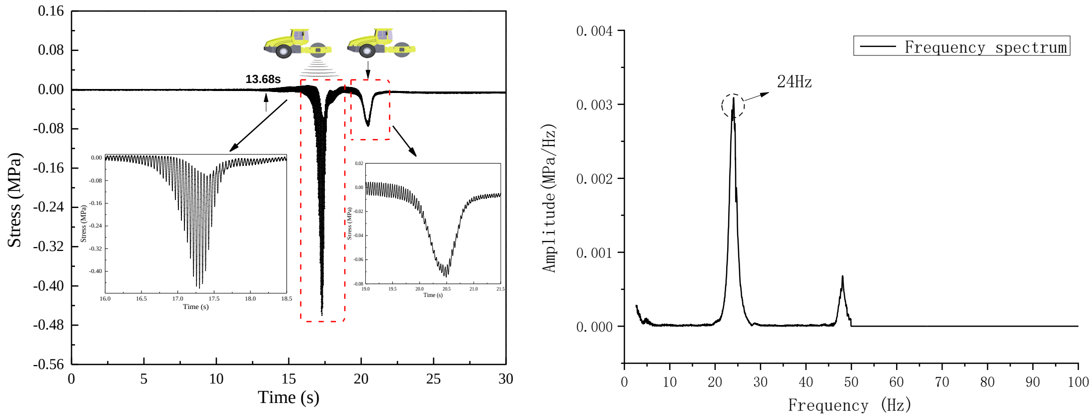

(a) Time history curve **(b) Frequency spectrum curve**

Fig. 7 Dynamic soil stress caused by moving roller

Fig. 8 presents the maximum dynamic soil stresses at different depths with the number of roller passes. For the test section TS-65 with thickness layer of 65 cm as shown in Fig. 8(a), the maximum dynamic soil stress at the depth of 15 cm increased from 0.50 MPa to 1.18 MPa, caused by the static compaction of 260 kN (by XS263J Roller) and dynamic compaction of 700 kN (by YZ362 Roller at 24 Hz) in the first two passes, respectively. Then the maximum dynamic soil stress decreased to 0.91 MPa and 0.55 MPa as the exciting force reduced to 500 kN (by YZ362 Roller at 21 Hz) and 260 kN (by XS263J Roller). It is obviously indicated that increased drum weight and vibratory frequency resulted in larger dynamic soil stresses. Besides, the dynamic soil stresses were observed to increase by 8.54% and 4.47% for the second compaction at the exciting forces of 700 kN and 500 kN, indicating that soils became densification to support more loads. Similar phenomenon also appeared in other soil depths as well as in the test section TS-80 with thickness layer of 80 cm as shown in Fig. 8(b). The maximum dynamic soil stresses at the depth of 18 cm were 0.46 MPa, 1.19 MPa and 0.89 MPa as the exciting forces varied from 260 kN to 700 kN and 500 kN consecutively. Increased roller passes led to the increments of dynamic soil stresses by 7.87% and 8.46% at the exciting force levels of 700 kN and 500 kN, respectively.

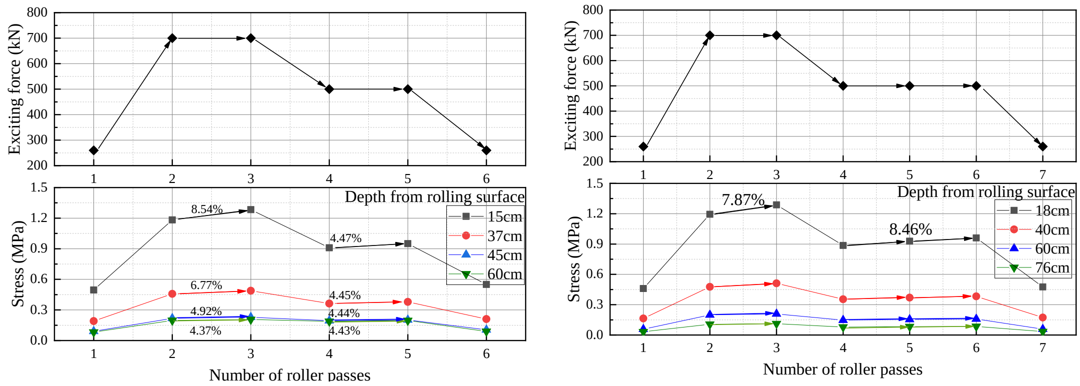

(a) TS-65 **(b) TS-80**

Fig. 8 Maximum dynamic soil stresses under different exciting forces

To further investigate the influencing depths of roller compaction, Fig. 9 presents the distributions of dynamic soil stresses along subgrade layers at different exciting forces. It can be found that dynamic soil stresses caused by the heavy vibratory rollers were 2.4~5.9 times larger than those of traditional rollers of 260 kN, especially at deeper depths. Dynamic soil stresses attenuated fast in the upper depth of 0.4~0.45 m, and then decreased slowly along subgrade depths. Although dynamic soil stresses reduced to only 0.032~0.107 MPa at the bottom of the compaction layer, they always located above the line of self-weight stress as shown in Fig. 9(a), which helped to ensure that the energy propagated by the vibratory roller penetrated through the entire thickness layer. It is stated that when dynamic soil stresses are lower than 20% of the subgrade self-weight stress, soils present almost elastic behavior and don't generate plastic deformation. On the contrary, subgrade soils could be densified in the full depth by all the three exciting forces. Meanwhile, dynamic soil stresses decreased from 0.50 MPa to 0.091 MPa within the depth of 0~0.45 m, with the reduction of almost 81.8% for the test section of TS-65. When the roller vibratory frequency increased to 21 Hz and 24 Hz with the exciting forces of 500 kN and 700 kN, dynamic soil stresses decreased from 0.91 MPa and 1.18 MPa to 0.19 MPa and 0.22 MPa with the reduction of 79.1% and 81.4%, respectively. It is interesting to notice that the attenuation rates of dynamic soil stresses were approximately similar for different exciting forces.

Fig. 9(b) shows the normalized stress $\boldsymbol{\sigma/P}$ decaying with subgrade depth, which presents independent relationship with the exciting forces. When the drum moves along the subgrade surface, the interface could be approximately assumed as a rectangular load with a length of 240 cm (*l*) and width of 15 cm (*b*). The Boussinesq's model is used to describe the distribution of dynamic soil stress as shown in Eq. (4) and Fig. 9(b). Since the surface pressure by the drum is distributed nonuniformly and the limited compaction thickness dose not satisfy the assumption of semi-infinite space, a dynamic stress attenuation coefficient k is introduced here to modify the Boussinesq's equation to describe the dynamic soil stress caused by roller loading:

$$\frac{\sigma_z}{P}(z) = k \cdot \frac{1}{2\pi bl} \cdot \left[\frac{mn}{\sqrt{1+m^2+n^2}} \cdot \left(\frac{1}{m^2+n^2} + \frac{1}{1+n^2}\right) + arctg\left(\frac{m}{n\sqrt{1+m^2+n^2}}\right)\right] \quad (4)$$

where, $m=l/b$, $n=z/b$. The lower and upper boundaries of dynamic soil stresses are provided at k=1.07 and 1.17 based on the 95% confidence analysis as shown in Fig.9 (b), which presented a good correlation with measured data.

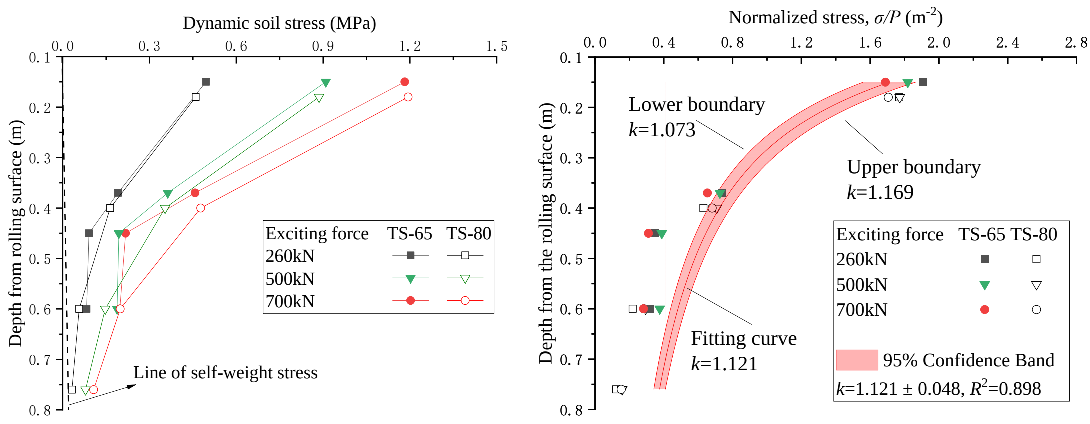

(a) Absolute values of dynamic soil stress **(b) Normalized soil stress**

Fig. 9 Distributions of dynamic soil stresses along subgrade layers

3.2 Compaction degree and settlement

Since the thickness layers of 65 cm and 80 cm were much larger than the traditional compaction layer, it is important to investigate the uniformity of compaction degree along the full subgrade depth. Based on the improved sand cone testing, Fig. 10 illustrates the results of compaction degree at three different layers for both TS-65 and TS-80, i.e., upper layer (first 1/3 depth), middle layer (middle 1/3 depth) and bottom layer (last 1/3 depth). Generally, soils were effectively compacted in a uniform fashion with respect to the full depth to 96%~97.2% and 94.1%~95.4% for the large thickness layers of 65 cm and 80 cm within limited 6~7 passes. However, the compaction degree at different soil depths exhibited quite different development characteristics with roller passes. For the test section of TS-65, it can be found that soils at the middle and bottom layers were densified quickly from initial values of 78.4%~78.5% to 93%~93.5% during the first three passes, especially under the exciting force of 700 kN. Then their compaction degree increased slowly to 96%~97.2% during the last three passes, where the compaction degree of the middle layer was 1.2% larger than that of the bottom layer. Although the dynamic soil stresses at the upper layers were much larger than those at deeper depths, the growth of soil compaction degree at upper layers lagged behind that at deeper subgrade depths, which kept linear increasing trend to 87.1% during the first three passes and then to 96.8% during the last three passes. It can be inferred that the dynamic stress level of 0.19 MPa at the bottom of thickness layer of 65 cm, caused by the exciting force of 500 kN, had the ability to compact soils to the desired compaction degree up to 96%. While for the upper layers, rollers with 260 kN exciting forces could compact soils to the desired compaction degree, which was consistent with the results of the test section of TS-30 by the traditional rollers. Moreover, soils at upper layers were difficult to be densified until the deeper layers were rigidly compacted. This phenomenon is similar to the compaction of hot asphalt mixtures introduced by Yan et al. (2021).

Therefore, it is important to provide enough support from the bearing layer before carrying out subgrade compaction.

In contrast, the growth characteristic of compaction degree of three different depths were approximately synchronous for the test section of TS-80, where the values of compaction degree increased quickly to 88.6%~90.3% during the first three passes under the exciting force of 700 kN and then grew slowly to 94.1%~95.4% during the three passes of 500 kN and one pass of 260 kN. Although the dynamic soil stresses at the upper and middle layers were close for sections of TS-65 and TS-80, the stress value at the bottom of TS-80 was only 0.079 MPa, about half of that for TS-65, which led to the corresponding compaction degree 1.9% lower than that of TS-65. Such insufficient compaction at the bottom layer further resulted in the relatively lower compaction degree at shallower depths. If the thickness layer increased larger than 80 cm, the full depth of subgrade might not be densified to the desired compaction degree.

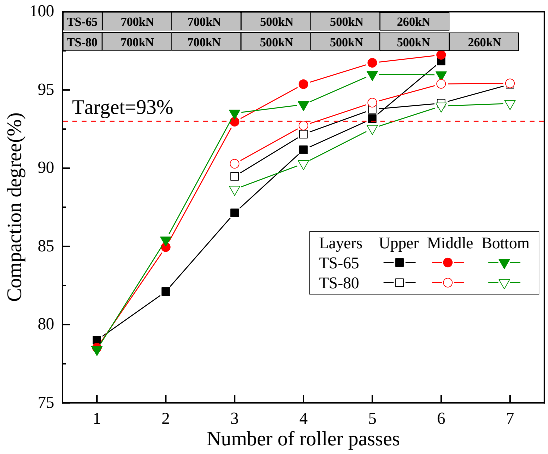

Fig. 10 Compaction degree of each layer with roller passes

The elevation measuring points were arranged every 5 m×20 m spacing in the test sections. Fig. 11 illustrates the accumulative settlement (*S*) and the relative difference (*RD*) of settlement between adjacent roller passes for test sections of TS-30, TS-65 and TS-80. The accumulative settlement presented an exponential growth trend, and their final values were 51.92 mm, 112.72 mm and 129.4 mm after 7, 6 and 7 roller passes for those three test sections. Considering the initial thickness layers of 30 cm, 65 cm and 80 cm, the coefficients of loose paving were determined to be 1.21, 1.21 and 1.19 in sequence. Larger coefficients represented better compaction quality for the same loose-paving subgrade. Therefore, the compaction effects of TS-30 and TS-65 were slightly better than that of TS-80, which was consistent with the results of compaction degree as shown in Fig. 10. Meanwhile, the relative difference (*RD*) of settlement decreased gradually with the roller passes, which was always considered as an index of stopping rolling with a critical value of 5 mm. According to this criterion, the recommended roller passes seemed to be 5, 4 and 5 for the thickness layers of 30 cm, 65 cm and 80 cm. However, the actual proper roller passes should be 5 and 6 based on the results of compaction degree as shown in Fig. 10. Therefore, for the subgrade filled with such poor-graded gravel (GP), the critical value of *RD* should be adjusted to 4 mm to satisfy the soil compaction degree along the full subgrade depth.

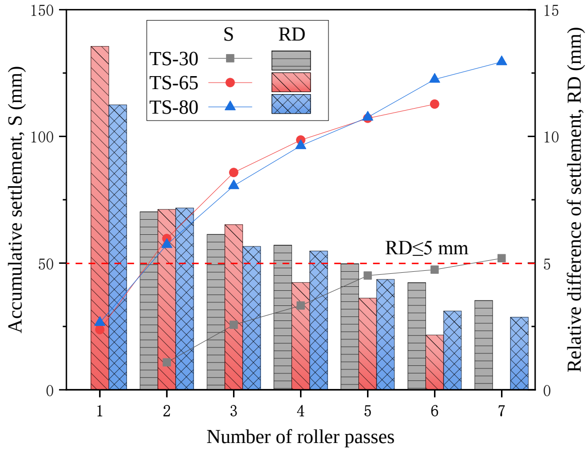

Fig. 11 Accumulative settlement and relative difference of settlement

3.3 Bearing capacity of compacted subgrade

Subgrade reaction modulus K_{30} is commonly used to evaluate the static bearing capacity of compacted soils. Fig. 12 plots the measured subgrade reaction modulus with roller passes for two large thickness layers in comparison to the conventional thickness of 30 cm. The K_{30} values increased approximately linearly with the roller passes, which reached about 188.2 MPa/m after six passes in TS-65 and 157.9 MPa/m after seven passes in TS-80, respectively. Since soils experienced better compaction in TS-65 than TS-80 as illustrated in Fig. 10, they presented stronger static bearing capacity in TS-65. As a contrast, the K_{30} value of TS-30 was about 160.7 MPa/m after seven passes, which was similar to that of TS-80. It can be inferred that heavy roller compacted subgrade with large thickness layers of 65 cm and 80 cm had equivalent even better static bearing capacity to that of conventional compaction thickness. Therefore, increasing thickness layer via heavy rollers is effective to replace the conventional technology to accelerate the construction earthworks.

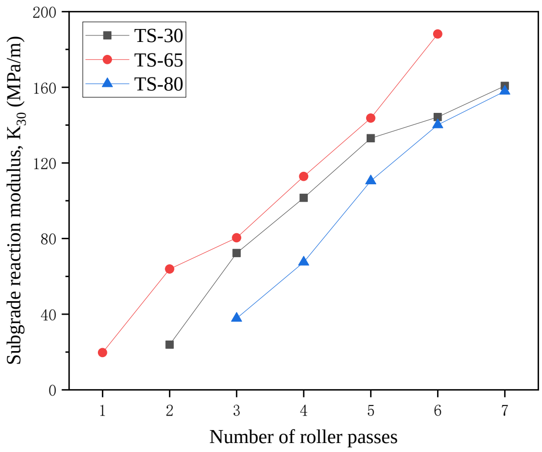

Fig. 12 Subgrade reaction modulus (K_{30})

Dynamic modulus of deformation E_{vd} is considered as an indicator to evaluate the dynamic bearing capacity of subgrade. Fig. 13 gives the measured dynamic modulus of deformation with roller passes for the three thickness layers. The E_{vd} values also increased approximately linearly with the roller passes as that of the K_{30} indicator, which finally reached about 62.8 MPa, 57.7 MPa and 67.3 MPa for TS-65 (six passes), TS-80 (seven passes) and TS-30 (seven passes), respectively. Different from the subgrade reaction modulus as shown in Fig. 12, the dynamic modulus of deformation of TS-65 was close to that of TS-30, both of which were larger than the values of 80 cm thick subgrade. Actually, the compacted subgrade exhibited high dynamic bearing capacities according to the criterions of 40 MPa required for the subgrade in high-speed railways.

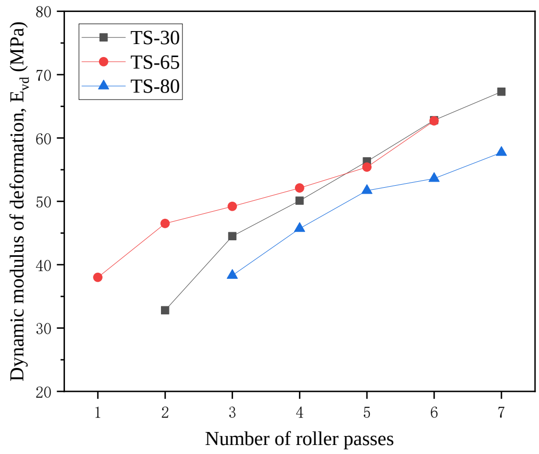

Fig. 13 Dynamic modulus of deformation (E_{vd})

The dynamic deflection L is the currently used acceptance indicator in highway subgrade. Fig. 14 presents the calculated dynamic deflection based on the Falling Weight Deflectometer (FWD) test, which decreased linearly to about 1.453 mm, 1.561 mm and 1.447 mm for TS-65, TS-80 and TS-30, respectively. According to the designed demand of 1.764 mm, the recommended roller passes would be 5, 6 and 6 for the thickness layers of 65 cm, 80 cm and 30 cm, which were in complete agreement with the results of compaction degree as shown in Fig. 10. Therefore, the indicator of dynamic deflection is more reliable to evaluate the compaction quality for large thickness layers than the indicators of subgrade reaction modulus and dynamic modulus of deformation.

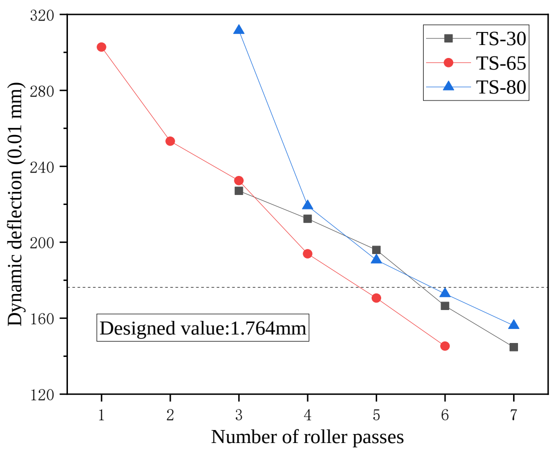

Fig. 14 Dynamic deflection based on the FWD test

3.4 Relationships between compaction degree and testing indicators

Although the compaction degree is the design index to directly judge the compaction quality, it is quite time-consuming to operate in the field measurement, especially for the subgrade with large thickness layers. Therefore, to establish the relationships between compaction degree and testing indicators, such as subgrade reaction modulus K_{30}, dynamic modulus of deformation E_{vd}, dynamic deflection L and relative difference of settlement RD, will be practical and convenient for the evaluation of roller compactions. Fig. 15 plots the relationships between soil compaction degree and these testing indicators for thickness layers of 65 cm and 80 cm, which could be empirically expressed by the following linear formulae as Eqs. (5)- (12).

Thickness layer of 65 cm:

$$\boldsymbol{K_{30} = 20.79 \pm 2.49K - 1826.71 \pm 234.39, R^2 = 0.921} \quad (5)$$

$$\boldsymbol{E_{vd} = 3.11 \pm 0.49K - 238.58 \pm 46.40, R^2 = 0.869} \quad (6)$$

$$\boldsymbol{L = -14.31 \pm 1.86K + 1527.93 \pm 176.21, R^2 = 0.922} \quad (7)$$

$$\boldsymbol{RD = -0.74 \pm 0.07K + 74.25 \pm 6.25, R^2 = 0.954} \quad (8)$$

Thickness layer of 80 cm:

$$\boldsymbol{K_{30} = 19.18 \pm 1.84K - 1682.35 \pm 170.75, R^2 = 0.932} \quad (9)$$

$$\boldsymbol{E_{vd} = 3.44 \pm 0.22K - 269.55 \pm 20.46, R^2 = 0.958} \quad (10)$$

$$\boldsymbol{L = -26.87 \pm 1.85K + 2705.36 \pm 172.30, R^2 = 0.963} \quad (11)$$

$$\boldsymbol{RD = -0.51 \pm 0.06K + 51.30 \pm 5.37, R^2 = 0.904} \quad (12)$$

Therefore, according to the designed target of compaction degree at 93%, the corresponding criterions of K_{30}, E_{vd}, L and RD are 107 MPa/m, 49 MPa, 1.97 mm and 5.1 mm for the thickness layer of 65 cm, and 122 MPa/m, 50 MPa, 1.92 mm and 3.8 mm for the thickness layer of 80 cm. If the designed targets of compaction degree increase to 94% or 96%, the corresponding criterions could also be determined from the proposed empirical formulae.

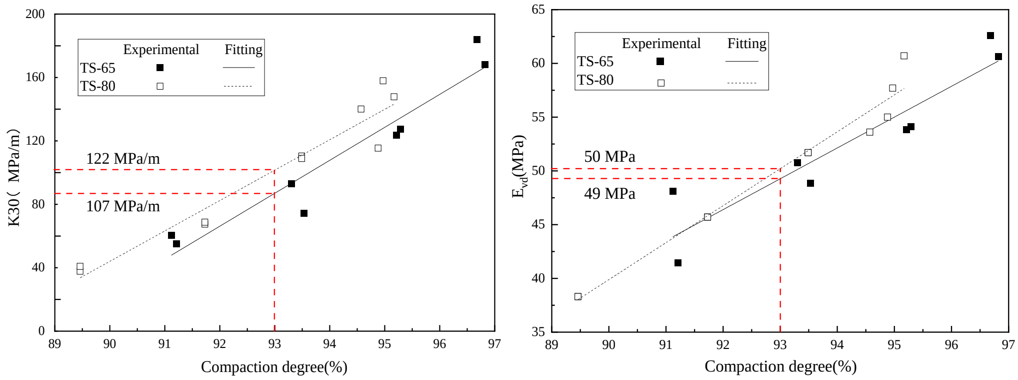

(a) K_{30} versus compaction degree **(b) E_{vd} versus compaction degree**

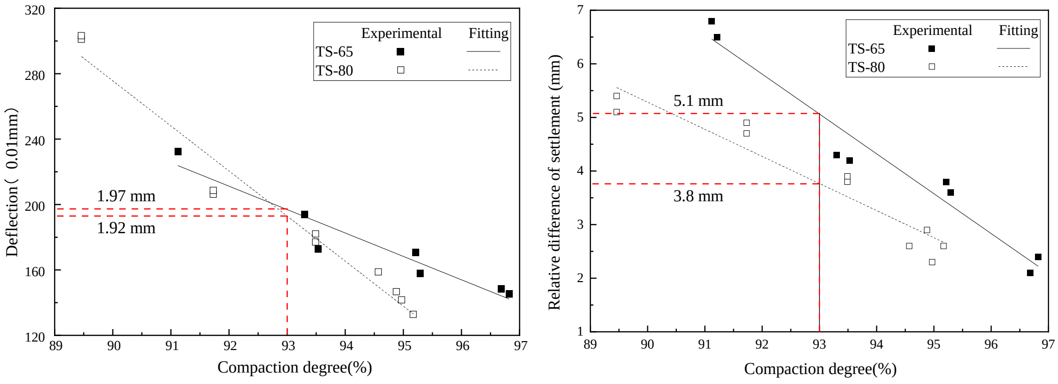

(c) Dynamic deflection versus compaction degree (d) Relative difference of settlement versus compaction degree

Fig. 15 Relationships between compaction degree and indicators

4 Conclusions

Full-scale field experiments were carried out to evaluate the compaction quality of gravel subgrade with large thickness layers of 65 cm and 80 cm via heavy vibratory rollers. The falling height in the sand cone test indeed influenced the measured sand density, which would underestimate the compaction degree at deeper soil depths for large thickness layers. Improved sand cone method was proposed and calibrated to investigate the distributions of soil compaction degree along the full subgrade depths. Dynamic soil stresses, accumulative settlement, indicators of subgrade bearing capacity were also measured with the roller passes, and their correlations with compaction degree were further analyzed to provide criterions to evaluate the compaction quality. Accordingly, the following conclusions can be drawn:

(1) Dynamic soil stresses caused by the heavy vibratory rollers at 21 Hz (500 kN) and 24 Hz (700 kN) were much larger than those of traditional rollers of 260 kN. The dynamic soil stresses in compacted layers could reach 0.19~1.18 MPa and 0.079~1.19 MPa for the thickness layers of 65 cm and 80 cm, which were large enough to densify the soils in the full depth. The attenuation of normalized stresses along soil depths was found independent on the exciting forces, and a unified empirical formula was proposed to determine the vertical distribution of dynamic soil stresses caused by roller excitation.

(2) Soils of the full subgrade depth could be compacted to 96%~97.2% and 94.1%~95.4% for the large thickness layers of 65 cm and 80 cm, which satisfied the design targets of 93%. However, the compaction degree at different soil depths exhibited quite different development characteristics with roller passes, which was mainly contributed to the compactness of deeper layers. Although the dynamic soil stresses at the upper layers were much larger than those at deeper depths, soils at upper layers were difficult to be densified until the deeper layers were rigidly compacted for the thickness layer of 65 cm. In contrast, the growth of compaction degree at three different depths were approximately synchronous for the thickness layer of 80 cm, but stayed in a relatively lower compaction state due to the insufficient compaction at the bottom layer. Therefore, it is important to provide enough support from the bearing layer to better densify the upper subgrade.

(3) Based on the comparisons of subgrade reaction modulus, dynamic modulus of deformation and dynamic deflection, heavy roller compacted subgrade with large thickness layers of 65 cm and 80 cm had equivalent even better bearing capacity to that of conventional compaction thickness. Therefore, increasing thickness layer via heavy rollers is effective to replace the conventional technology to accelerate the construction earthworks. Moreover, the indicator of dynamic deflection is more reliable to evaluate the compaction quality for large thickness layers than the indicators of subgrade reaction modulus and dynamic modulus of deformation.

(4) A series of empirically linear formulae were established between soil compaction degree and subgrade reaction modulus, dynamic modulus of deformation, dynamic deflection and relative difference of settlement to conveniently evaluate the compaction qualities. Corresponding compaction criterions of K_{30}, E_{vd}, L and RD were suggested for the designed targets of compaction

degree at 93% for the thickness layers of 65 cm and 80 cm. It can be concluded that increasing thickness layer via heavy rollers could significantly reduce the cost and time burdens involved in construction while ensuring overall subgrade quality. And these relationships are beneficial to the quality control of intelligent compaction in the future research.

Acknowledgements

Financial supports from the National Natural Science Foundation for Young Scientists of China (Grant No. 51608306), Shandong Natural Science Foundation (Grant No. ZR2021ME103, ZR2021QE254), Shandong Transportation Science and Technology Foundation (2020-MS1-044, 2021B63, 202060804178), and Young Scholar Future Plan Funds of Shandong University are gratefully acknowledged.

References

ASTM (American Society for Testing Materials), 2017. Standard Practice for Classification of Soils for Engineering Purposes (Unified Soil Classification System), D2487-2017. US-ASTM.

Chen AJ, Su CH, Tang XYN, 2019. Construction technology of large thickness vibratory compaction of hard rock embankment. *E3S Web of Conferences*, **136**: 04025. https://doi.org/10.1051/e3sconf/201913604025

Chen Y, Jaksa MB, Kuo YL, Scott BT, 2021. Discrete element modelling of the 4-sided impact roller. *Computers and Geotechnics*, **137**: 104250. https://doi.org/10.1016/j.compgeo.2021.104250

Cui XZ, 2010. Real-Time diagnosis method of compaction state of subgrade during dynamic compaction. *Geotechnical Testing Journal*, **33**(4): 299 - 303. https://doi.org/10.1520/GTJ102268

Fujyu T, Sugawara J, Takuno H, Okano H, 2004. Load and deflection measurement for evaluation of ground strength with portable FWD system. SICE 2004 Annual Conference, p. 489 - 492. https://doi.org/10.11499/SICEP.2004.0_48_3

Ghanbari E, Hamidi A, 2014. Numerical modeling of rapid impact compaction in loose sands. *Geomechanics and Engineering*, **6**(5): 487 – 502. http://doi.org/10.12989/gae.2014.6.5.487

Kim K, 2010. Numerical simulation of impact rollers for estimating the influence depth of soil compaction. MS Thesis, Texas A&M University, Texas, America.

Kim K, Chun S, 2016. Finite element analysis to simulate the effect of impact rollers for estimating the influence depth of soil compaction. *KSCE Journal of Civil Engineering*, **20**(7): 2697 - 2701. https://doi.org/10.1007/s12205-016-0013-8

Li RK, Che AL, Feng SK, 2020. Electrical measurement based laboratory testing method of physical properties of subgrade soil. *Journal of Engineering Geology*, **28**(1): 51 – 59 (in Chinese). https://doi.org/10.13544/j.cnki.jeg.2019-187

Mohammed MM, Roslan H, Firas S, 2013. Assessment of rapid impact compaction in ground improvement from in-situ testing. *Journal of Central South University*, **20**(3): 786 – 790. http://doi.org/10.1007/s11771-013-1549-0

Mooney MA, Rinehart RV, 2007. Field monitoring of roller vibration during compaction of subgrade soil. *Journal of Geotechnical and Geoenvironmental Engineering*, **133**(3): 257 - 265. https://doi.org/10.1061/(ASCE)1090-0241(2007)133:3(257)

MTPRC (Ministry of Transport of the People's Republic of China), 2015. Specifications for Design of Highway Subgrades, JTG D30 - 2015. China Communications Press, Beijing, China (in Chinese).

MTPRC (Ministry of Transport of the People's Republic of China), 2019. Technical Specifications for Construction of Highway Subgrades, JTG/T 3610 - 2019. China Communications Press, Beijing, China (in Chinese).

MTPRC (Ministry of Transport of the People's Republic of China), 2019. Filed Test Method of Highway Subgrade and Pavement, JTG 3450 - 2019. China Communications Press, Beijing, China (in Chinese).

MTPRC (Ministry of Transport of the People's Republic of China), 2020. Test Methods of Soils for Highway Engineering, JTG 3430 - 2020. China Communications Press, Beijing, China (in Chinese).

MTPRC (Ministry of Transport of the People's Republic of China), 2019. Filed Test Method of Highway Subgrade and Pavement, JTG 3450 - 2019. China Communications Press, Beijing, China (in Chinese).

NRAPRC (National Railway Administration of the People's Republic of China), 2018. Standard for Acceptance of Earthworks in High-speed Railway, TB 10751-2018. China Railway Publishing House, China (in Chinese).

Sulewska MJ, 2012. The control of soil compaction degree by means of LFWD. *Baltic Journal of Road and Bridge Engineering*, **7**(1): 36 – 41. https://doi.org/10.3846/bjrbe.2012.05

Vennapusa PKR, White DJ, 2009. Comparison of light weight deflectometer measurements for pavement foundation materials. *Geotechnical Testing Journal*, **32**(3): 239 - 251. https://doi.org/10.1520/GTJ101704

Vennapusa PKR, White DJ, Siekmeier J, Embacher RA, 2012. In situ mechanistic characterisations of granular pavement foundation layers. *International Journal of Pavement Engineering*, **13**(1): 52 – 67. https://doi.org/ 10.1080/10298436.2011.564281

Wersaell C, Larsson S, 2013. Small-scale testing of frequency-dependent compaction of sand using a vertically vibrating plate. *Geotechnical Testing Journal*, **36**(3): 394 - 403. https://doi.org/10.1520/GTJ20120183

Wersaell C, Nordfelt I, Larsson S, 2017. Soil compaction by vibratory roller with variable frequency. *Géotechnique*, **67**(3): 272 - 278. https://doi.org/10.1680/jgeot.16.P.051

Wersaell C, Nordfelt I, Larsson S, 2018. Resonant roller compaction of gravel in full-scale tests. *Transportation Geotechnics*, **14**: 93 - 97. https://doi.org/10.1016/j.trgeo.2017.11.004

Wersaell C, Nordfelt I, Larsson S, 2020. Roller compaction of rock-fill with automatic frequency control. *Proceedings of the Institution of Civil Engineers - Geotechnical engineering*, **173**(4): 339 - 347. https://doi.org/10.1680/jgeen.19.00159

Xu BB, 2021. Quality inspection method of layered compacted subgrade and engineering example analysis. *E3S Web of Conferences*, **248**: 03068. https://doi.org/10.1051/e3sconf/202124803068

Xu C, Chen ZQ, Li JS, Xiao YY, 2013. Compaction of subgrade by high-energy impact rollers on an airport runway. *Journal of Performance of Constructed Facilities*, **28**(5): 4014021. https://doi.org/10.1061/(ASCE)CF.1943-5509.0000469

Yan TH, Marasteanu M, Le JL, 2021. One-dimensional nonlocal model for gyratory compaction of hot asphalt mixtures. *Journal of Engineering Mechanics*, **148**(2): 04021144. https://10.1061/(ASCE)EM.1943-7889.0002073

Yuan GL, Che AL, Feng SK, 2020. Evaluation method for the physical parameter evolutions of highway subgrade soil using electrical measurements. *Construction and Building Materials*, **231**: 117162. https://doi.org/10.1016/j.conbuildmat.2019.117162

Zhang ZP, Zhou ZJ, Guo T, Xu TY, Zhu LX, Xu F, Chen CR, Liu T, 2021. A measuring method for layered compactness of loess subgrade based on hydraulic compaction. *Measurement Science and Technology*, **32**(5): 055106. https://doi.org/10.1088/1361-6501/abd7ab